Progress In Electromagnetics Research, Vol. 141, 645–657, 2013

MULTI-BAND CIRCULAR POLARIZER USING ARCHIMEDEAN SPIRAL STRUCTURE CHIRAL METAMATERIAL WITH ZERO AND NEGATIVE REFRACTIVE INDEX

Liyun Xie, Helin Yang*, Xiaojun Huang, and Zhenjun Li

College of Physical Science and Technology, Central China Normal University, Wuhan 430079, China

Abstract—A novel multi-band circular polarizer is proposed by using a bilayered chiral metamaterial (CMM). The unit cell of the CMM is composed of four Archimedean spiral structures, which are twisted 90° to each other in the upper and bottom layers. When a linearly polarized wave incidents on this circular polarizer, the simulation result shows that the transmission of right circularly polarized (RCP) wave can be obtained at 14.28 GHz and 15.96 GHz, while the transmission of left circularly polarized (LCP) wave is emitted at 15.3 GHz and 16.88 GHz. The retrieval results reveal that the effective refractive index of the CMM closes to zero or negative at the vicinity of four resonances. The experimental results are in good agreement with the numerical results.

1. INTRODUCTION

Metamaterials (MMs) are artificial composite materials and can exhibit special electromagnetic (EM) properties which do not exist in natural materials [1–3]. Based on the MMs, arbitrary values of effective permittivity and permeability can be designed, so one can design some amazing function device such as perfect lens [4] and invisible cloaking [5]. In recent years, the research in chiral metamaterials (CMMs) has been growing rapidly due to their special electromagnetic properties which are optical activity and circular dichroism [6–12]. On the strength of these peculiarities, CMMs have been proposed to manipulate polarization states of electromagnetic waves for achieving polarization rotation [13–29]. For example, a CMM pattern composed

Received 30 June 2013, Accepted 30 July 2013, Scheduled 5 August 2013

* Corresponding author: He-Lin Yang (emyang@mail.ccnu.edu.cn).

of twisted four U-shaped split ring resonators with negative refractive index has been proposed [28], which transforms incident linearly polarized waves into circularly polarized waves with different directions of rotation at two distinct resonances. However, as a circular polarizer, it has relatively low polarization extinction ratio and polarization conversion efficiency. Recently, Cheng et al. [15] studied a double-layered split ring resonator structure to get a LCP and RCP wave with relatively high polarization conversion efficiency, but only single-band LCP and RCP wave can be obtained by this CMM. In order to increase the resonant frequency, multi-band circular polarizer by using multi-layered planar spiral array has been reported [17, 21]. In addition, other chiral structures have been reported, such as cross chiral structure [18, 22], rose pirouette structure [23–25], conjugated gammadions structure [26], and so on. All these structures can exhibit circular dichroism and optical activity with negative index.

In this paper, we proposed a multi-band asymmetric CMM using a double-layered Archimedean spirals array in which the bottom spirals twist 90° compared to the upper spirals. In the unit cell, two pairs of Archimedean spirals with different parameters are adopted to construct the whole circular polarizer. The structure is novel due to Archimedean spiral is intrinsic chirality, so the design is combined intrinsic chirality with structure chirality. When a y-polarized EM wave is incident on the proposed sample, it is found that relatively pure circularly polarized wave can be obtained in transmission at four resonance frequencies. S parameters retrieval results show that at three resonant frequencies the effective refraction index is close to zero [30], and the other is negative refraction index. The transformation coefficient from a linearly polarized wave to a circularly polarized wave is relatively high with respect to most of the negative refraction index CMMs that have been reported [13, 21, 27]. The proposed multi-band polarizer has simple geometry and is easily fabricated with conventional printed circuit board technology, and can be used in applications such as laser [31, 32], antenna [33–35], and remote sensors.

2. THEORETICAL ANALYSIS

Chiral metamaterials are made of unit cells without any mirror symmetry so that the cross-coupling between electric and magnetic fields exists at the resonance. Therefore, RCP wave and LCP wave would encounter different transmission coefficients. The chiral medium can be represented by the chirality parameter κ. Thus, the constitutive relations in the CMMs are written as [10]

$$\mathbf{D} = \varepsilon_0\varepsilon\mathbf{E} + i\kappa\sqrt{\mu_0\varepsilon_0}\mathbf{H}, \quad \mathbf{B} = \mu_0\mu\mathbf{H} - i\kappa\sqrt{\mu_0\varepsilon_0}\mathbf{E} \tag{1}$$

where ε_0 and μ_0 are the permittivity and permeability of vacuum; ε and μ are the relative permittivity and permeability of the CMMs. Electromagnetic field of chiral medium can be stated as

$$\mathbf{E} = \mathbf{E}_+ + \mathbf{E}_-, \quad \mathbf{H} = \mathbf{H}_+ + \mathbf{H}_-, \quad \mathbf{H}_\pm = \pm i\mathbf{E}_\pm/\eta. \tag{2}$$

The electric fields of RCP (+) wave and LCP (−) wave are defined as $\mathbf{E}_\pm$; $\eta = \sqrt{\mu_0\mu/\varepsilon_0\varepsilon}$ is wave impedance of CMMs. According to Maxwell's equations and constitutive relations we can get wave equation of $\mathbf{E}_\pm$

$$\left(\nabla^2 + k_\pm^2\right)\mathbf{E}_\pm = 0 \tag{3}$$

where $k_\pm = n_\pm k_0$, $k_0 = \omega/c$ is the free-space wave number vector; $n_\pm$ are the refractive indexes of RCP and LCP wave, which are given by:

$$n_\pm = n \pm \kappa \tag{4}$$

where $n = \sqrt{\varepsilon\mu}$. From formula (4), clearly, given a large enough chirality, the negativity of n_+ or n_- is possible, when n is approximately $-\kappa$, n_+ approximates to zero, and when n is approximately κ, n_- approximates to zero. Based on this principle, we can design negative refraction index or near-zero refraction index chiral metamaterials with circular dichroism and optical activity, which can realize polarization rotate of electromagnetic wave.

3. DESIGN, SIMULATION, AND EXPERIMENT

The unit cell of the CMM is depicted in Figure 1(a), which is composed of two pairs of the Archimedean spirals, and the spirals in diagonal are identical. The parameters of the spirals by No. 2 are scaled down by a factor of 0.9 with respect to the parameters of the spirals marked by No. 1. The spirals on the back side of the substrate are twisted 90° with respect to the spirals on the front side. The dielectric lamina is chosen to be Arlon AD 250 with relative permittivity of 2.5 and loss tangent of 0.003. The thickness of the lamina is $t = 2.1$ mm, and the copper pattern has a thickness of 0.03 mm. The period constant of the CMM is represented by parameter a. The following geometric parameters are used in the simulation and experiment: $a = 10$ mm, $r = 0.2$ mm, $w = 0.85$ mm and $g = 0.3$ mm.

We started the analysis with numerical simulation of the CMM structure using CST Microwave Studio which is based on the finite difference time domain (FDTD) method. The boundaries are selected to be periodic in the x and y directions and open the z direction. A y-polarized wave propagating along $+z$ direction is employed as the excitation source. Due to the lack of C4 symmetric [36] in this

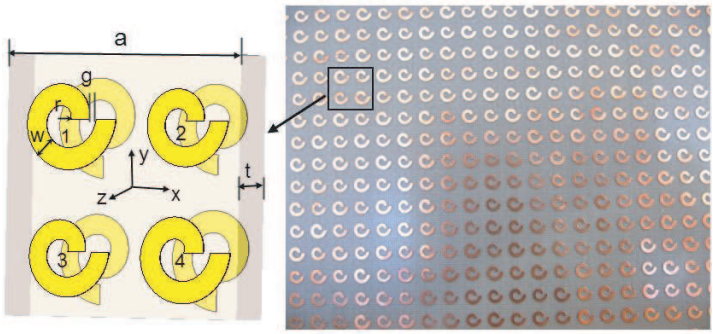

Figure 1. Schematic of designed CMM structure: (a) a unit cell geometry of simulated (b) a photo of the experimental sample.

CMM, the response to the incident electric field along x direction is different from y direction. In this work, y direction is chosen. In the experiment, the chiral structure with a dimension of 15×15 unit cells was fabricated, shown as Figure 1(b). A standard linearly polarized double-ridge horn antenna is utilized as the transmitter while a planar LCP antenna and a planar RCP antenna are employed as the receiver in turn. The prototype is placed in the middle between the antennas. The transmission coefficient measurements are performed using a vector network analyzer of Agilent PNA E8362B. The transmission of circularly polarized waves also can be converted from the linear transmission coefficients co-polarization T_{yy} and cross-polarization T_{xy}, $T_{\pm} = T_{xy} \pm iT_{yy}$, where the subscript "+" indicates the RCP wave, and the subscript "−" indicates the LCP wave.

4. RESULTS AND DISCUSSION

Numerical and experimental circular transformation coefficients for the RCP and LCP components are presented in Figures 2(a) and (b). There are four obviously transmission peaks in the frequency band ranging from 13 GHz to 18 GHz. The simulated results reveal that the transmission of the LCP wave reaches its minimum value at 14.28 GHz and 15.96 GHz, and the transmission coefficients are −40.23 dB and −23.29 dB, respectively. The minimum contributions of the RCP component are observed at 15.3 GHz as −29 dB, and at 16.88 GHz as −28 dB. It follows the feature of circular polarizer that studied CMM originates from the different circular polarization transformation coefficients for the RCP and LCP components, due to a y-polarized

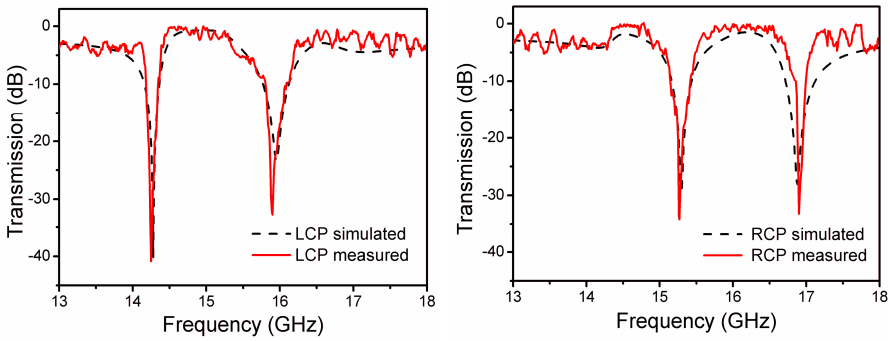

Figure 2. Numerical and experimental results for the circular transformation coefficients. (a) LCP wave, (b) RCP wave.

incident wave. One of the circular polarizations is eliminated at the resonance frequencies, whereas the other polarization is transmitted with a small loss. As a result, at 14.28 GHz and 15.96 GHz, the transmitted wave is RCP. Similarly, at 15.3 GHz and 16.88 GHz, the LCP wave is transmitted.

The measured results are in good agreement with the simulated ones. Due to the fabrication and measurement tolerance, the four measured transmission gaps have slight shift with respect to simulation. We can note that the transmission coefficients are both less than -30 dB at these four resonances, and the measured transmission coefficients are -3.3 dB at 14.25 GHz, -0.54 dB at 15.9 GHz, which are the resonances of RCP wave; -1.78 dB at 15.27 GHz, and -2.5 dB at 16.9 GHz, which are the resonances of LCP wave.

In order to understand the role that two pairs of spirals of array play in the CMM, the transmission characteristics of the unit cell with only the twisted spirals 1 (2) are calculated, and the results are depicted in Figure 3. For the case of the only twisted spirals 1, the bigger one, there are two obviously resonant frequencies in the range of 14–15.5 GHz, which are the LCP and RCP wave, respectively. For the case of the only twisted spirals 2, the smaller one, it can be observed that, the obvious difference between the transmission of LCP and RCP wave in the frequency range 15.5–17 GHz. Based on the above results, it can draw a conclusion that the bigger twisted spirals play an important role at the lower frequencies, while the smaller ones are responsible for the polarization rotation at the higher frequencies.

The ratio of the cross-polarization transmission and co-polarization transmission $|T_{xy}|/|T_{yy}|$ and the phase difference $\phi(T_{xy}) -$

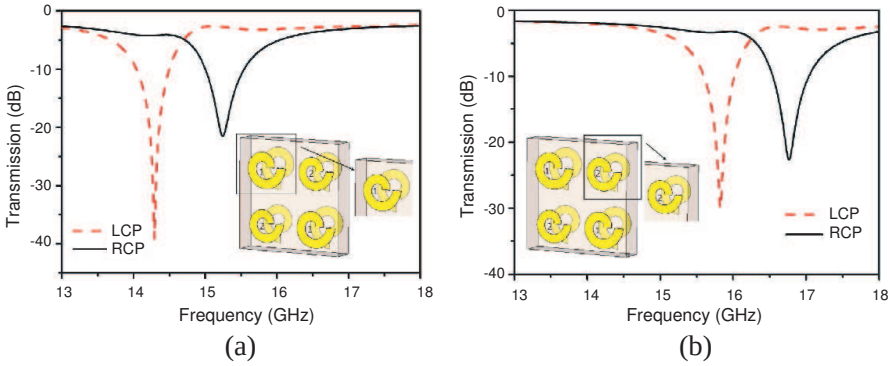

Figure 3. Transmission of LCP and RCP of the unit cell for the only twisted (a) spirals 1 and (b) spirals 2.

$\phi(T_{yy})$ can also demonstrate the polarization characteristics of the transmitted wave. Figure 4(a) shows the corresponding result. It can be seen that the values of ratio $|T_{xy}|/|T_{yy}|$ and phase difference are 0.98 and 91.8° at 14.28 GHz, 1.06 and −91.7° (268.3°–360°) at 15.3 GHz, 1.18 and 92.34° at 15.96 GHz, 0.92 and −88.27° at 16.88 GHz. The above results indicate that the rotations of the transmitted field are right-handed at 14.28 GHz and 15.96 GHz, which are then changed to left-handed at 15.3 GHz and 16.88 GHz. In addition it can be found that the emitted fields are close to the pure circularly polarized wave at these resonant frequencies, which is in good agreement with the results of the circular transmission in Figure 2.

In order to clearly demonstrate the optical activity of the polarization rotator, polarization azimuth rotation angle θ and ellipticity η are calculated by the following formulas [37]

$$\theta = \frac{1}{2}\left[\arg(T_+) - \arg(T_-)\right], \tag{5}$$

$$\eta = \frac{1}{2}\sin^{-1}\left\{\frac{|T_+|^2 - |T_-|^2}{|T_+|^2 + |T_-|^2}\right\} \tag{6}$$

The polarization azimuth rotation angle θ denotes the rotation angle between the polarization planes of the emitted and incident waves, while the ellipticity η represents the polarization state of the emitted wave. When η equals to zero, the emitted wave is a linearly polarized wave that the polarization plane has a rotation angle of θ relative to the incident wave, which indicates pure optical activity is produced. The emitted wave would be circularly polarized if η equals to ±45°. Figure 4(b) shows the simulated results of the polarization azimuth

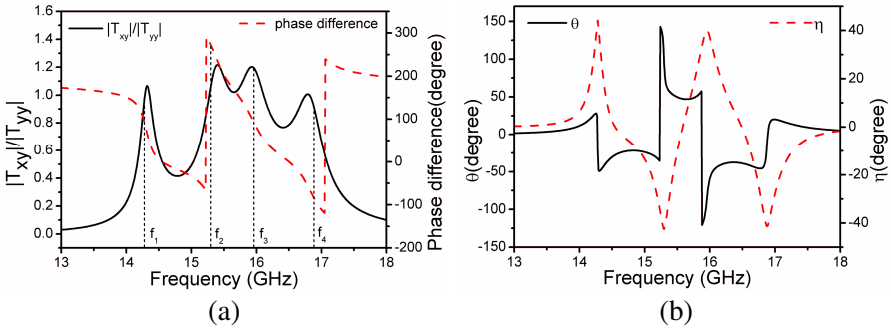

Figure 4. Simulated results for the CMM: (a) The ratio of $|T_{xy}|/|T_{yy}|$ and phase difference of $\phi(T_{xy}) - \phi(T_{yy})$. (b) Polarization azimuth rotation angle θ and ellipticity η of the CMM.

rotation angle θ and ellipticity η of the transmitted wave. It can be clearly seen that, the value of η is 44.1° at 14.28 GHz, −42.5° at 15.3 GHz, 40° at 15.96 GHz, −41.4° at 16.88 GHz. It means the transmitted fields are close to pure circular polarization. In addition, it also can be seen that the values of ellipticity η are in the vicinity of 0° at 14.5 GHz, 15.5 GHz and 16.5 GHz, the polarization rotation angle θ are −27.6°, 47.4° and −38.6°, respectively, which corresponds a optical activity effect. It indicates that the polarization plane of the emitted wave has −27.6°, 47.4° and −38.6° rotation with respect to the incident wave, respectively.

Figure 5 shows the retrieved effective parameters of the CMM based on the simulated S parameters. In the Figure 5(a), the value of κ and n are: $n_1 = 1.44$, $\kappa_1 = 1.35$, $n_2 = 1.26$, $\kappa_2 = -1.23$, $n_3 = -1.14$, $\kappa_3 = 3.31$, $n_4 = 0.64$, $\kappa_4 = -0.41$, at the four resonant frequencies in the order from the low frequency to the high frequency. Using the formula (4), we calculate the refractive index of LCP wave $n_{1-} = n_1 - \kappa_1 = 0.09$, $n_{3-} = n_3 - \kappa_3 = -4.45$, at the frequency 1 and frequency 3, the refractive index of RCP wave $n_{2+} = n_2 + \kappa_2 = 0.03$, $n_{4+} = n_4 + \kappa_4 = 0.23$; at the frequency 2 and frequency 4, as shown in Figure 5(b). The results indicate that for the LCP and RCP wave of the proposed CMM, the refraction index is close to zero or negative due to strong chirality parameter κ; and the real parts of the retrieved effective permittivity ε and permeability μ are presented in Figure 5(c).

The mechanism of resonances for the four Archimedes spirals CMM can be understand by studying the surface current distributions on the upper and bottom layer, as shown in Figure 6. For the first two resonant frequencies of 14.28 GHz and 15.3 GHz, the strong surface

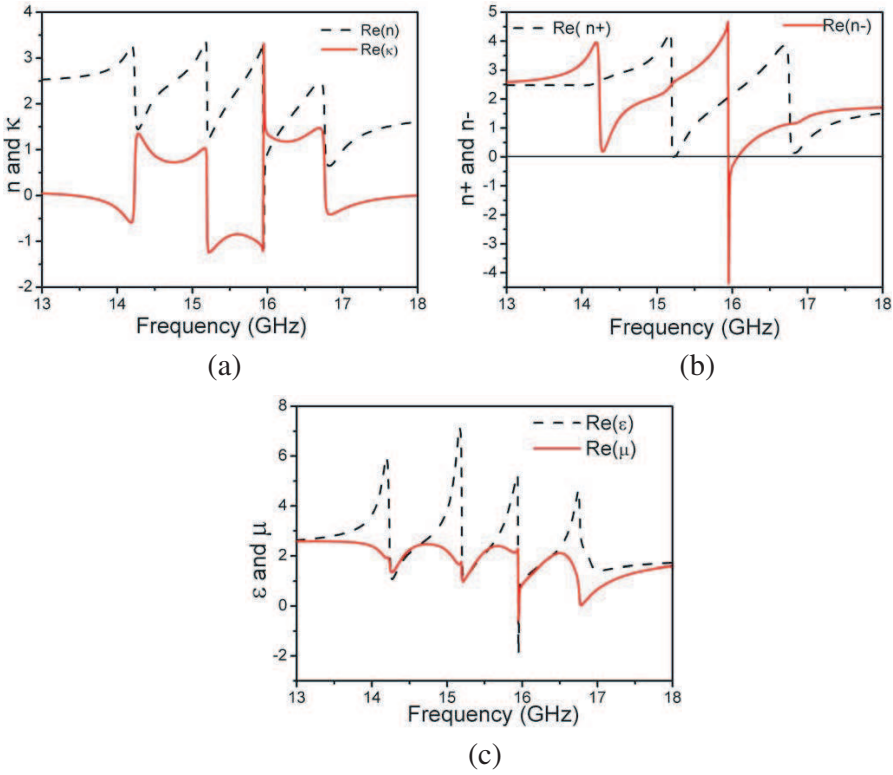

Figure 5. The retrieved effective parameters of the CMM based on the simulated S parameters. (a) The real parts of the effective refractive index n and chirality κ. (b) The real parts of refractive index for LCP and RCP waves Re $(n+)$ and Re $(n-)$. (c) The real parts of the permittivity ε and permeability μ.

current is induced on the lager spirals, while relatively weak current energy exists on the smaller ones, as denoted in Figures 6(a), (b), which means the RCP and LCP wave caused by the lager spiral array in the whole sample. Furthermore, the directions of the surface currents on the upper and bottom layers are identical at 14.28 GHz, which exhibits some characteristics similar to electric dipole and generates electric resonance [38]; the directions of the surface currents on the upper and bottom layers are opposite at 15.3 GHz, which exhibits some characteristics similar to magnetic dipole and generates magnetic resonance. The same analysis is also applicable to the second resonant frequencies of the RCP and LCP wave, which the surface

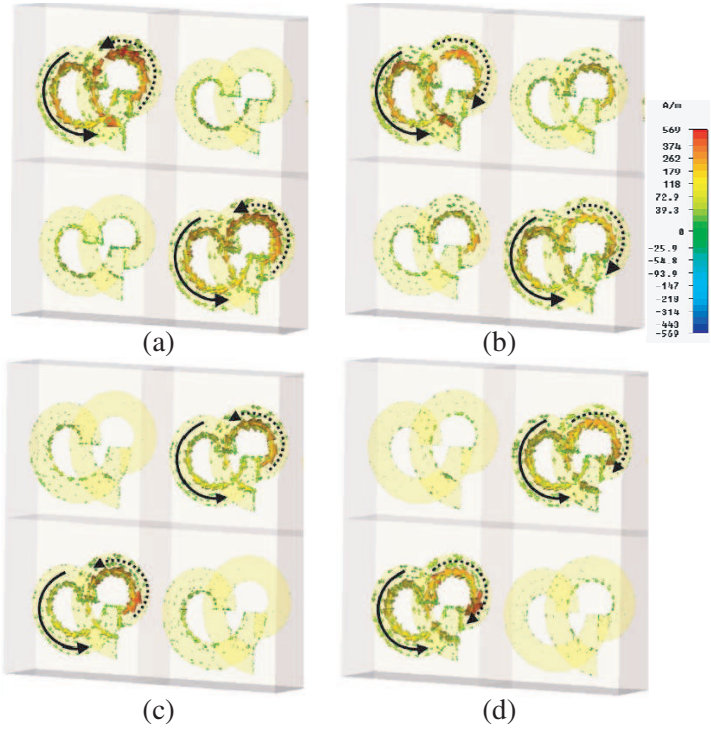

Figure 6. Surface current distribution at (a) 14.28 GHz, (b) 15.3 GHz, (c) 15.96 GHz, and (d) 16.88 GHz.

currents are mainly distributed in the smaller spirals, as denoted in Figures 6(c), (d). Due to the different forms of resonance in the CMM, the RCP wave and LCP wave emerge different transmission coefficients, and then the strong optical activity is obtained.

5. CONCLUSION

In conclusion, a multi-band CMM based on Archimedean spiral structures is proposed. Both simulation and experiment results have demonstrated that circular polarization wave is obtained at four frequencies, when a y-polarized wave incidents on this sample. The effective refractive index of RCP or LCP is close to zero or negative at the vicinity of the resonances. The surface current distribution is studied to understand that the larger twisted spirals array plays the great role in the CMM at the lower frequency while the twisted spirals array with smaller size is responsible for the higher polarization

rotation frequency. The design has multiple-frequency bands which can be utilized as a circular polarizer for microwave applications and have much potential application in the microwave domain.

REFERENCES

1. Burlak, G., "Spectrum of Cherenkov radiation in dispersive metamaterials with negative refraction index," *Progress In Electromagnetics Research*, Vol. 132, 149–158, 2012.
2. Sabah, C., H. T. Tastan, F. Dincer, K. Delihacioglu, M. Karaaslan, and E. Unal, "Transmission tunneling through the multi-layer double-negative and double-positive slabs," *Progress In Electromagnetics Research*, Vol. 138, 293–306, 2013.
3. Canto, J. R., C. R. Paiva, and A. M. Barbosa, "Dispersion and losses in surface waveguides containing double negative or chiral metamaterials," *Progress In Electromagnetics Research*, Vol. 116, 409–423, 2011.
4. Pendry, J. B., "Negative refraction makes a perfect lens," *Phys. Rev. Lett.*, Vol. 85, No. 18, 3966–3969, 2000.
5. Schurig, D., J. J. Mock, B. J. Justice, S. A. Cummer, J. B. Pendry, A. F. Starr, and D. R. Smith, "Metamaterial electromagnetic cloak at microwave frequencies," *Science*, Vol. 314, No. 5801, 977–980, 2006.
6. Gansel, J., M. Thiel, M. S. Rill, M. Decker, K. Bade, V. Saile, G. von Freymann, S. Linden, and M. Wegener, "Gold helix photonic metamaterial as broadband circular polarizer," *Science*, Vol. 325, No. 5947, 1513–1515, 2009.
7. Li, J., F.-Q. Yang, and J.-F. Dong, "Design and simulation of L-shaped chiral negative refractive index structure," *Progress In Electromagnetics Research*, Vol. 116, 395–408, 2011.
8. Zhao, R., T. Koschny, and C. M. Soukoulis, "Chiral metamaterials: Retrieval of the effective parameters with and without substrate," *Opt. Express*, Vol. 18, No. 14, 14553–14567, 2010.
9. Decker, M., R. Zhao, C. M. Soukoulis, S. Linden, and M. Wegener, "Twisted split-ring-resonator photonic metamaterial with huge optical activity," *Opt. Lett.*, Vol. 35, No. 10, 1593–1595, 2010.
10. Wang, B., J. Zhou, T. Koschny, M. Kafesaki, and C. M. Soukoulis, "Chiral metamaterials: Simulations and experiments," *J. Opt. A: Pure Appl. Opt.*, Vol. 11, 114003, 2009.
11. Sabah, C. and H. G. Roskos, "Design of a terahertz polarization rotator based on a periodic sequence of chiral-metamaterial and

dielectric slabs," *Progress In Electromagnetics Research*, Vol. 124, 301–314, 2012.

12. Cao, T. and M. J. Cryan, "Circular dichroism in planar nonchiral metamaterial made of elliptical nanoholes array," *Journal of Electromagnetic Waves and Applications*, Vol. 26, No. 10, 1275–1282, 2012.
13. Mutlu, M., A. E. Akosman, A. E. Serebryannikov, and E. Ozbay, "Asymmetric chiral metamaterial circular polarizer based on four U-shaped split ring resonators," *Opt. Lett.*, Vol. 36, No. 9, 1653–1655, 2011.
14. Huang, C., J. Zhao, T. Jiang, and Y. Feng, "Asymmetric transmission of linearly polarized electromagnetic wave through chiral metamaterial structure," *Journal of Electromagnetic Waves and Applications*, Vol. 26, Nos. 8–9, 1192–1202, 2012.
15. Cheng, Y., Y. Nie, L. Wu, and R. Z. Gong, "Giant circular dichroism and negative refractive index of chiral metamaterial based on split-ring resonators," *Progress In Electromagnetics Research*, Vol. 138, 421–432, 2013.
16. Song, K., X. P. Zhao, Q. H. Fu, Y. H. Liu, and W. R. Zhu, "Wide-angle 90°-polarization rotator using chiral metamaterial with negative refractive index," *Journal of Electromagnetic Waves and Applications*, Vol. 26, Nos. 14–15, 1967–1976, 2012.
17. Ma, X., C. Huang, M. B. Pu, Y. Q. Wang, Z. Y. Zhao, C. T. Wang, and X. G. Luo, "Dual-band asymmetry chiral metamaterial based on planar spiral structure," *Appl. Phys. Lett.*, Vol. 101, 161901–161904, 2012.
18. Zhou, J., J. Dong, B. Wang, T. Koschny, M. Kafesaki, and C. M. Soukoulis, "Negative refractive index due to chirality," *Phys. Rev. B*, Vol. 79, 121104–4, 2009.
19. Zarifi, D., M. Soleimani, and V. Nayyeri, "A novel dual-band chiral metamaterial structure with giant optical activity and negative refractive index," *Journal of Electromagnetic Waves and Applications*, Vol. 26, Nos. 2–3, 251–263, 2012.
20. Wu, Z., B. Q. Zhang, and S. Zhong, "A double-layer chiral metamaterial with negative index," *Journal of Electromagnetic Waves and Applications*, Vol. 24, No. 7, 983–992, 2010.
21. Ma, X., C. Huang, M. B. Pu, C. G. Hu, Q. Feng, and X. G. Luo, "Multi-band circular polarizer using planar spiral metamaterial structure," *Opt. Express*, Vol. 20, No. 14, 16050–16058, 2012.
22. Dong, J., J. Zhou, T. Koschny, and C. Soukoulis, "Bi-layer cross chiral structure with strong optical activity and negative refractive

index," *Optics Express*, Vol. 17, No. 16, 14172–14179, 2009.

23. Plum, E., J. Zhou, J. Dong, V. A. Fedotov, T. Koschny, C. M. Soukoulis, and N. I. Zheludev, "Metamaterial with negative index due to chirality," *Phys. Rev. B*, Vol. 79, No. 3, 035407(6), 2009.
24. Rogacheva, A. V., V. A. Fedotov, A. S. Schwanecke, and N. I. Zheludev, "Giant gyrotropy due to electromagnetic-field coupling in a bilayered chiral structure," *Phys. Rev. Lett.*, Vol. 97, 177401, 2006.
25. Plum, E., V. A. Fedotov, A. S. Schwanecke, N. I. Zheludev, and Y. Chen, "Giant optical gyrotropy due to electromagnetic coupling," *Appl. Phys. Lett.*, Vol. 90, No. 22, 223113, 2007.
26. Zarifi, D., M. Soleimani, and V. Nayyeri, "Dual-band multiband chiral metamaterial structures with strong optical activity and negative refraction index," *IEEE Antennas and Wireless Progagation Letters*, Vol. 11, 334–337, 2012.
27. Ye, Y., X. Li, F. Zhuang, and S. W. Chang, "Homogeneous circular polarizers using a bilayered chiral metamaterial," *Appl. Phys. Lett.*, Vol. 99, No. 3, 031111, 2011.
28. Li, Z., R. Zhao, T. Koschny, M. Kafesaki, K. B. Alici, E. Colak, H. Caglayan, E. Ozbay, and C. M. Soukoulis, "Chiral metamaterials with negative refractive index based on four "U" split ring resonators," *Appl. Phys. Lett.*, Vol. 97, No. 8, 081901(3), 2010.
29. Ranga, Y., L. Matekovits, S. G. Hay, and T. S. Bird, "An anisotropic impedance surface for dual-band linear-to-circular transmission polarization convertor," *IEEE International Workshop on Antenna Technology, (IWAT2013)*, 47–50, 2013.
30. Zhou, B., H. Li, X. Y. Zou, and T.-J. Cui, "Broadband and high-gain planar vivaldi antennas based on inhomogeneous anisotropic zero-index metamaterials," *Progress In Electromagnetics Research*, Vol. 120, 235–247, 2011.
31. Nejadmalayeri, A. and P. R. Herman, "Ultrafast laser waveguide writing: Lithium niobate and the role of circular polarization and picosecond pulse width," *Opt. Lett.*, Vol. 31, 2987–2989, 2006.
32. Nasimuddin, X. Qing, and Z. N. Chen, "Compact circularly polarized symmetric-slit microstrip antennas," *IEEE Trans. on Antennas and Propagat.*, Vol. 59, No.1, 285–288, 2011.
33. Sze, J., K. L. Wong, and C. C. Huang, "Coplanar waveguide-fed square slot antenna for broadband circularly polarized radiation," *IEEE Trans. on Antennas and Propagat.*, Vol. 51, No. 8, 2141–

2144, 2003.

34. Kasabegoudar, V. G. and K. J. Vinoy, "A broadband suspended microstrip antenna for circular polarization," *Progress In Electromagnetics Research*, Vol. 90, 353–368, 2009.
35. Zarifi, D., H. Oraizi, and M. Soleimani, "Improved performance of circularly polarized antenna using semi-planar chiral metamaterial covers," *Progress In Electromagnetics Research*, Vol. 123, 337–354, 2012.
36. Liseikina, T. and A. Macchi, "Features of ion acceleration by circularly polarized laser pulses," *Appl. Phys. Lett.*, Vol. 91, No. 17, 171502, 2007.
37. Huang, C., X. L. Ma, M. B. Pu, G. W. Yi, Y. Q. Wang, and X. G. Luo, "Dual-band 90° polarization rotator using twisted split ring resonators array," *Optics Communications*, Vol. 291, 345, 2013.
38. Liu, N., H. Liu, S. Zhu, and H. Giessen, "Stereometamaterials," *Nat. Photon.*, Vol. 3, 157, 2009.